



A novel technique for the humidity dependent calibration of hypoiodous acid (HOI) and iodine (I₂)

Lewis Marden¹, Marvin D. Shaw¹, Stephen J. Andrews¹, Maya Zmajkovic¹, Phil Rund², Becky Alexander², Joel Thornton², Andrew Peters³, Lucy J. Carpenter¹

¹Wolfson Atmospheric Chemistry Laboratories, Department of Chemistry, University of York, Heslington, York, YO10 5DD, UK

²Department of Atmospheric and Climate Sciences, University of Washington

³Bermuda Institute of Ocean Sciences, St George's, Bermuda

Correspondence to: Lewis Marden (lewis.marden@york.ac.uk), Lucy Carpenter (lucy.carpenter@york.ac.uk), Marvin Shaw (marvin.shaw@york.ac.uk)

Abstract. Hypoiodous acid (HOI) and molecular iodine (I₂) are important precursors of reactive gaseous iodine, which plays an important role in the oxidative capacity of the atmosphere and in aerosol formation in the marine boundary layer. HOI and I₂ are emitted from the ocean surface and recycled on atmospheric aerosol via heterogeneous chemistry. Measurements of these molecules, which are typically present in the marine boundary layer at the low-to-sub part per trillion (ppt) level, are sparse, in part due to difficulties in quantification with a lack of appropriate instrumentation and calibration techniques. A novel calibration technique is developed for HOI via generation from I₂ hydrolysis and then 1:1 conversion of HOI back to I₂ through a NaI trap, allowing the sensitivity of HOI to be calculated relative to I₂, which is readily calibrated using a permeation tube system. Using this calibration method, we describe the use of a reduced pressure high resolution chemical ionisation mass spectrometer (CIMS) to characterise the sensitivities of HOI and I₂ over a range of humidities representative of the marine boundary layer and to measure these molecules in the field. At humidities of over 50% RH, the CIMS sensitivity of I₂ is humidity independent whereas HOI exhibits a slight negative humidity dependence. The effect of inlet interactions on HOI and I₂ signals is investigated, with HOI observed to convert to I₂. The implications of these inlet interactions and humidity sensitivities for future ambient measurement configurations are discussed.

1 Introduction

Iodine species play an important role in atmospheric chemistry and climate. They influence the oxidative capacity of the atmosphere through the destruction of ozone (O₃) (Chameides and Davis, 1980; Solomon et al., 1994; Read et al., 2008; Saiz-Lopez et al., 2014; Sherwen et al., 2016a) and alteration of hydrogen oxides (HO_x) and nitrogen oxides (NO_x) cycles (Simpson et al., 2015; Saiz-Lopez and Von Glasow, 2012). They can also oxidize elemental mercury (Calvert and Lindberg, 2004;



Auzmendi-Murua et al., 2014; Lee et al., 2024) and are involved in new particle formation, with iodine oxide radicals (IO), produced during the reaction between O_3 and iodine, self-reacting and further ozonising to form I_2O_5 which can hydrolyse to form HIO_3 (O'dowd et al., 2002; Sipilä et al., 2016; Finkenzeller et al., 2023).

Of the halogens, iodine has the most profound impact on tropospheric O_3 cycling and significantly modifies the atmospheric response to anthropogenic perturbations of ozone precursor emissions. Global model simulations show that atmospheric iodine chemistry lowers the global tropospheric O_3 burden by 6–20% and reduces O_3 concentrations by several parts per billion (ppb), with significant effects over polluted and populated regions (Saiz-Lopez et al., 2014; Sherwen et al., 2016a; Sherwen et al., 2016b; Wang et al., 2021b; Pound et al., 2023; Caram et al., 2023). The dominant source of atmospheric iodine is from the oceans, primarily from the reaction of O_3 and iodide on the sea surface (Garland et al., 1980; Carpenter et al., 2013; Macdonald et al., 2014), resulting in the emission of molecular iodine (I_2) and hypoiodous acid (HOI). HOI is thought to be the largest source, representing $\approx 75\%$ of iodine emissions into the troposphere (Sherwen et al., 2016a). In the atmosphere, I_2 and HOI rapidly photolyse, producing reactive iodine radicals that catalytically destroy O_3 (Saiz-Lopez and Von Glasow, 2012; Simpson et al., 2015). This cycle represents a negative feedback mechanism, whereby increased O_3 concentrations are offset by increased iodine emissions (Carpenter et al., 2013; Prados-Roman et al., 2015). In fact, model calculations project that future increases in anthropogenic O_3 will be buffered by iodine (Iglesias-Suarez et al., 2020), which has implications for future air quality. Ice core records have shown that there has been a tripling of atmospheric iodine since 1950 (Cuevas et al., 2018; Legrand et al., 2018), likely due to increased anthropogenic O_3 production. Recent measurements of iodine radicals in the lower stratosphere (Koenig et al., 2020) have also demonstrated the potential for iodine to contribute to stratospheric ozone depletion. Iodine has a far higher O_3 destruction potential than chlorine (Klobas et al., 2021) and has been implicated as a potential reason for the unexplained decrease in extra-polar lower stratospheric O_3 (Koenig et al., 2020), which is a region where O_3 changes exert strong radiative effects on climate (Neale et al., 2025).

Despite the significance of HOI and I_2 as the main emission source of atmospheric iodine, and of HOI as a sink for the iodine oxide (IO) radical, there have been few measurements of these compounds. Measurements of I_2 , which has been detected by both Differential Optical Absorption Spectroscopy (DOAS) and by Chemical Ionisation Mass Spectrometry (CIMS), have typically been restricted to coastal areas (Saiz-Lopez and Plane, 2004; Bitter et al., 2005; Peters et al., 2005; Mahajan et al., 2009; Huang et al., 2010) with only one measurement in the remote ocean region (Lawler et al., 2014). There has so far been only one directly quantified measurement of HOI, by CIMS, also in a coastal region rather than the open ocean (Tham et al., 2021). There are several challenges that contribute to the scarcity of measurements of these molecules. The mixing ratios of iodine compounds are low, in the sub-ppt to 10 ppt range over the ocean, due to their short atmospheric lifetimes (Saiz-Lopez et al., 2012; Lawler et al., 2014). In addition, halogen compounds can undergo heterogeneous chemistry on the surfaces of instrument inlets, resulting in loss or potentially addition of signal (Neuman et al., 2010; Liao et al., 2012; Liao et al., 2014; Le Breton et al., 2017; Peng et al., 2022). Further, there is a lack of highly sensitive and selective measurement techniques and



instrumentation to measure and quantify these compounds. Given that reactive halogen chemistry is increasingly being incorporated into global chemistry transport models, there is an urgent requirement for observations to help provide constraints and improve model capabilities.

Chemical ionisation mass spectrometry is increasingly being used in the measurement of trace atmospheric gases due to its high sensitivity and selectivity, high time-resolution, soft ionisation, and ability to directly measure compounds in the field with minimal sample preparation (Huey, 2007; Lee et al., 2014; Zhang et al., 2023; Riva et al., 2024). Reagent ions are generated and interact with sample molecules in an ion molecule reactor (IMR) to produce analyte ions, such as through charge transfer or adduct formation reactions. Various reagent ions have been used to measure atmospheric halogen species such as SF_5^- to measure HCl and ClONO_2 (Marcy et al., 2005), NO_3^- to measure HIO_3 (Sipilä et al., 2016; Finkenzeller et al., 2023), and SF_6^- to measure bromine and chlorine compounds such as Br_2 , Cl_2 , BrCl , IBr , and BrO (Sjostedt and Abbatt, 2008; Buys et al., 2013; Roscoe et al., 2014). More recently, I^- has been used for a wide range of chlorine and bromine atmospheric species including Cl_2 , Br_2 , ClONO_2 , BrNO_2 , ClONO_2 , ClO , BrO , HCl , HOCl , HOBr , BrCl , and various chlorine-containing OVOCs (Kercher et al., 2009; Lee et al., 2014; Custard et al., 2016; Le Breton et al., 2017; Lee et al., 2018; Priestley et al., 2018). However, the I^- reagent ion is not effective in measuring trace levels of iodine species as they can be formed during the generation of the reagent gas (Wang et al., 2021a). An alternative is to use Br^- as a reagent ion. This has previously been used to measure Cl_2 , HO_2 , H_2SO_4 and HNO_3 (Lawler et al., 2011; Sanchez et al., 2016; Rissanen et al., 2019; Wang et al., 2020) and more recently to detect various iodine species such as I_2 , HOI , ICl and IBr using a chemical ionisation atmospheric pressure interface time-of-flight (CI-API-TOF) mass spectrometer (Tham et al., 2021; Wang et al., 2021a; He et al., 2023). A reduced pressure Br-CIMS has also been developed which can produce analyte ions through an AIM (adduct ionisation mechanism) IMR (Riva et al., 2024). The instrument operates at medium pressures (50–500 mbar) producing low electric fields ($E/N < 10$ Td or field-free conditions), which reduces the chances of fragmentation and promotes adduct formation as the primary method of analyte formation. This loses some of the sensitivity compared to higher pressure CIMS instruments due to the reduced numbers of collisions occurring in the IMR. However, this is compensated for with an increased linear range of detected compounds through promotion of adduct formation.

It has previously been shown that water can form an adduct with halide (I^- , Br^-) reagent ions (R1), which can subsequently act as a reagent ion itself (R3) (Lee et al., 2014; Wang et al., 2021a). The formation enthalpy between a sample molecule and the hydrated reagent ion is lower than with the dry reagent ion (He et al., 2023), and so increasing humidity should result in a decrease in sensitivity, as the proportion of dry reagent ions decreases. However, for small molecules (<8 atoms), increasing humidity has generally been shown to increase sensitivity (Lee et al., 2014; Iyer et al., 2016). This was explained by Quantum Rice-Ramsperger-Kassel (QRRK) theory (Rice and Ramsperger, 1927; Kassel, 1928) which treats the halide adduct cluster as a collection of harmonic oscillators at an identical frequency. The cluster will fragment if energy above a critical threshold is localised in a single oscillator. Adding a water molecule to the cluster increases the number of harmonic oscillators, which



decreases the probability that the critical energy threshold is reached in a single oscillator (Kurtén et al., 2010), resulting in a decrease in the rate of fragmentation of the newly formed clusters (R4 and R5). Additionally, a lower energy fragmentation pathway is available for the hydrated adduct (R6), which kicks out the water molecule and keeps the sample molecule and reagent ion together.



where *A* is the sample molecule.

This kinetic enhancement via the water molecule is in competition with the thermodynamic effect of lower formation enthalpy and will affect different sample molecules to different degrees, requiring the humidity dependence of every molecule of interest to be quantified. Additionally, the humidity dependence will vary between instruments due to differences in IMR conditions and instrument tuning settings.

In this work, the ability for the Br-CIMS to detect and quantify the iodine species I_2 and HOI is demonstrated, and the impact of changing humidity on the instrument sensitivity to these molecules is quantified.

2 Methods

2.1 Bromide Time-of-Flight Chemical Ionisation Mass Spectrometry (CIMS)

The measurement of I_2 and HOI were performed using a Vocus S Chemical Ionisation Time-of-Flight (CI-TOF) Mass Spectrometer (ToFwerk, Switzerland), a high resolution ($R \approx 5000$) instrument that can produce Br^- reagent ions and Br-adduct analyte ions through a Vocus Aim reactor. The operational principles of the instrument and the AIM reactor are described in detail by Riva et al. (2024).

The Br^- reagent ions are generated by passing 0.25 SLPM ultra-high purity N_2 gas over a permeation tube held at 80 °C containing >99% benzene, C_6H_6 , and trace amounts of bromoethane, $\text{C}_2\text{H}_5\text{Br}$. This gas mixture is passed into a vacuum ultraviolet (VUV) ion source where UV light is emitted from a Kr lamp at 116.487 nm and 123.584 nm which is absorbed by



the benzene, generating photoelectrons (R7) (Ji et al., 2020; Breitenlechner et al., 2022). These photoelectrons react with the C_2H_5Br , generating Br^- ions (R8) (Riva et al., 2024).



The Br^- reagent ions are passed into an ion-molecule reactor (IMR) where it is joined by 1.8 SLPM of sample gas which has been passed into the sampling inlet and through a 0.475 mm critical orifice. The IMR is temperature controlled at 50 °C and pressure controlled at 50 mbar using a vacuum pump (IDP3, Agilent Technologies). The Br^- reacts with sample molecules to form adduct ions. These are drawn through another critical orifice and travel through four differentially pumped chambers which remove neutral molecules and focus the ions into a narrow beam before entering the drift region of the time-of-flight (ToF) chamber. Ions in the TOF chamber are extracted in discrete packets at a frequency of 18.02 kHz and converted into mass spectra using an MCP detector with a preamplifier over a range of 7–510 Th. The extracted packets are averaged over a period of 1 second which is also the speed of data collection. Data averaging, mass calibration, peak assignment, peak fitting and peak integration were all performed using the software package Tofware (version 4.0.1, Aerodyne Research Inc.) used in Igor Pro 9 software (Wavemetrics). This data was then exported and analysed further using the R language for statistical computing (R Core Team).

2.2 Humidity generation

The calibrations performed in this work were made over a humidity range from near complete dryness to almost 100% RH in order to be able to correct for effects caused by variations in ambient humidity in field measurements. This was achieved by humidifying the N_2 gas entering the instrument to various degrees using an in-house dynamic liquid calibration unit (LCU). The operation of this liquid calibration system has been described elsewhere (Yeoman et al., 2022) but is briefly covered here. The LCU is comprised of a proportional liquid-gas mixing valve (Bronkhorst) which controls the mass flow of liquid measured by a mini-Coriolis flow meter (Bronkhorst). It introduces a mass flow controlled zero-air dilution gas to aerosolize and fully evaporate the liquid into a temperature-controlled mixing region. The liquid is pressurized without gas contact, using a custom-built pneumatic cylinder with wetted materials of glass and PTFE.

The gas output of the LCU was maintained at 3.5 SLPM and the water concentration ranged from 0–5 g h⁻¹. During the I_2 calibrations, an additional flow of N_2 gas was used to dilute the humidified flow further. The tubing between the LCU outlet and the additional flow was heated to prevent saturation and condensation of the water vapour.



2.3 Calibration setup

2.3.1 I₂ calibration

An I₂ permeation tube was constructed by adding solid I₂ crystals (99.99%, Sigma-Aldrich) into a ¼” o.d. thin-walled PFA tube with the ends heat sealed closed. The permeation tube was held at 40 ± 0.1 °C and was continuously swept by 20 sccm high-purity oxygen-free N₂ gas. The emission rate was calculated gravimetrically by measuring the mass loss of the permeation tube over several months and corresponded to an emission rate of 34.7 ± 0.21 ng min⁻¹. Humidified N₂ gas from the LCU was used to dilute the permeation gas flow. The CIMS internal sample pump was used to sample the diluted I₂ permeation gas. The quantity of dilution flow used for the calibrations was varied by altering the speed of the sample pump, with excess dilution gas from the LCU flowed through an overflow port. Using different pump speeds altered the concentration of I₂, allowing for calibration curves to be constructed at different humidity levels. Concentrations of I₂ used during the calibrations ranged from 1–3 × 10¹⁰ molecules cm⁻³ (600–1000 ppt at SATP).

2.3.2 HOI calibration

HOI was generated from the hydrolysis of I₂ (R9) in an experimental setup similar to that previously developed for the generation of HOBr in a study by Liao et al. (2012). 500 sccm of N₂ gas was passed over the same I₂ permeation tube from the I₂ calibration and mixed with 500 sccm N₂ gas which had been humidified by passing through a bubbler containing Milli-Q water. This was passed over wetted AgNO₃ crystals (99% Fluorochem) in a 9.5 cm long ½” o.d. PFA tube. A small aqueous layer forms on the AgNO₃ crystal surface, in which I₂ hydrolysis occurs (R9). The AgNO₃ reacts with the generated I⁻ and H⁺ (R 10–12), pushing the (R9) equilibrium in favour of HOI production.



The resulting I₂ and HOI gas mixture was diluted by humidified N₂ gas from the LCU before being drawn into the CIMS at a flow rate of ≈ 4.1 SLPM. The AgNO₃ reactor tube and instrument inlet were wrapped in heating tape and heated to 50 °C to avoid HOI loss to the tube and inlet walls. The quantification of HOI is achieved by the inclusion of a trap containing sodium iodide (NaI) crystals (99%, Sigma-Aldrich). When the trap is in place, HOI is converted back into I₂ (R13).





The sensitivity of HOI relative to I_2 was found by comparing the HOI signal loss and I_2 signal gain from R13. A 1:1 conversion of HOI to I_2 was assumed, consistent with the approach of Liao et al. (2012) for the equivalent HOBr–Br₂ system. Figure 1 shows the simplified schematic of the calibration and an idealised example of the relative change between I_2 and HOI.

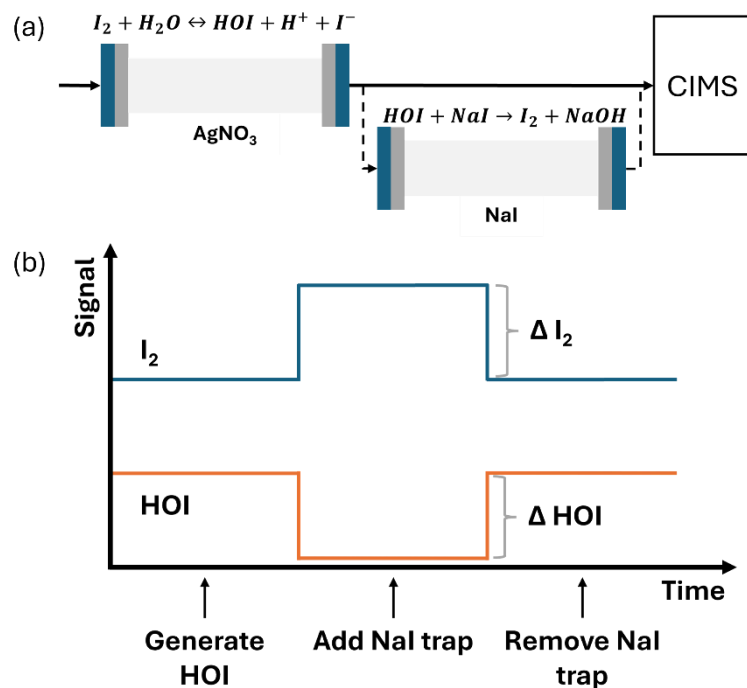


Figure 1: (a) A simplified schematic of the HOI calibration setup with reactions shown for HOI generation and destruction. (b) An idealised example of the change in HOI and I_2 signal in the CIMS on addition and removal of the NaI trap.

2.4 Field measurements at Tudor Hill Marine Atmospheric Observatory, Bermuda

The CIMS instrument was deployed during the Bermuda boundary Layer Experiment on the Atmospheric Chemistry of Halogens (BLEACH) field campaign in June 2022. The instrument was stationed at the Tudor Hill Marine Atmospheric Observatory (THMAO) on the west coast of the island of Bermuda (32.26° N, 64.88° W). At this site, the instrument was placed on top of a temporary sampling tower at 10 metres above ground level and 40 metres above sea level. The instrument was contained in an air-conditioned water-resistant enclosure and located at the top of the tower, minimising the potential for inlet effects to occur. The sample inlet was a short (15 cm, ½ in. outer diameter) length of PFA tube. A PTFE guard was placed at the entrance of the inlet tube, with an opening at the bottom, orientated 90° to the inlet. This allowed air to enter at a 90° bend and continue to the instrument while reducing the number of particles entering the CIMS as they impact onto the inlet



walls. The sampling rate was 4.1 L min^{-1} , resulting in an inlet residence time of 0.59 s. The Reynolds number was 155, indicating laminar flow once the air was past an 8.5 cm entrance length.

3. Results and Discussion

3.1 Detection of iodine compounds

I_2 and HOI were detected as adducts with Br^- , with the two $\text{I}_2\cdot\text{Br}^-$ isotopes observed at m/Q 332.73 and 334.73 Th and the two $\text{HOI}\cdot\text{Br}^-$ isotopes at 222.83 and 224.83 Th. The single peak mass spectra fits are shown in Fig. 2, taken from an HOI calibration experiment and of ambient air at Tudor Hill, Bermuda. At the instrument resolution of 5000, the high mass defect of the $\text{I}_2\cdot\text{Br}^-$ adduct allows it to be clearly differentiated from other peaks at 333 m/Q as seen in Fig. 2 d–f, even during ambient conditions at low mixing ratios. The $\text{HOI}\cdot\text{Br}^-$ adduct has a smaller mass defect, and subsequently has more overlap with interferent peaks. During the HOI generation stage of the calibration (Fig 2a), the HOI signal is significantly greater than any interferent peaks. However, on addition of the NaI trap (Fig 2b), or during ambient measurements (Fig 2e), the HOI signal overlaps with other interferent peaks. Despite this, the resolution is sufficient for Tofware’s multi-peak fitting algorithm (Stark et al., 2015) to identify HOI even at very low mixing ratios. Detection limits during field conditions are discussed in section 3.7.

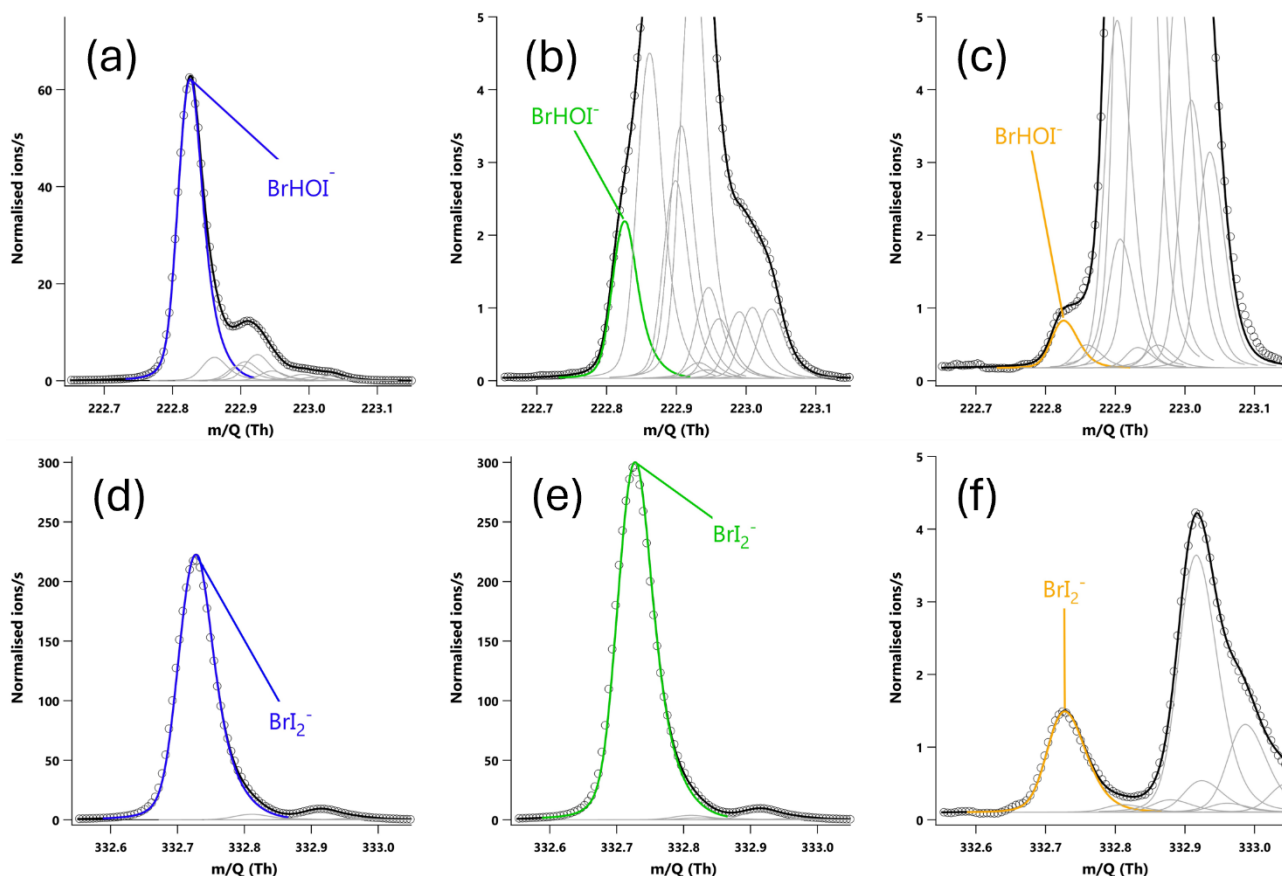


Figure 2: 20-minute averaged high resolution single peak mass spectra fits for HOI (a,b,c) and I₂ (d,e,f). The signal intensities correspond to mixing ratios of (a) 60.8 ppt, (b) 2.2 ppt, (c) 0.87 ppt, (d) 190.2 ppt, (e) 254.0 ppt and (f) 1.37 ppt. (a) The signal of HOI and (d) I₂ during an HOI calibration run without the NaI trap. (b) The signal of HOI and (e) I₂ during an HOI calibration run on addition of the NaI trap. (c) Ambient air measurements of HOI and (f) I₂ in a high humidity environment.

3.2 Signal normalisation

The I₂ and HOI adducts are formed from a pseudo first order reaction between the sample molecules and the Br⁻/H₂OBr⁻ reagent ions, and the adduct signal intensity is proportional to the reagent ions available. During experiments, the quantity of available reagent ions fluctuates over time. This can be due to variations in the efficiency of the ion source in generating the reagent ions, or with slight changes within the instrument. This variation can be corrected for by normalising the analyte signal against the sum of the reagent ions measured by the instrument, shown in Eq. (1). For CIMS instruments, the normalised signal is typically reported per million reagent ions, with units of normalised counts per second per million reagent ion counts per second (ncps).



$$\text{Normalised signal (ncps)} = \frac{A \cdot \text{Br}^- (\text{cps})}{\text{Br}^- (\text{cps}) + \text{H}_2\text{OBr}^- (\text{cps})} * 10^6 \quad (1)$$

where A is the sample molecule

3.3 I₂ humidity dependence

The humidity of the instrument IMR, where the reagent ion collisions occur, is not directly measured but has been related to the sample relative humidity (Wang et al., 2021a; He et al., 2023) and/or vapour pressure of water (Lee et al., 2014; Lee et al., 2018). An alternative method is to use the ratio between the first reagent ion water cluster, H₂OBr⁻, and the dry reagent ion, Br⁻ (Dörich et al., 2021), Eq. (2). This has the advantage of not requiring further equipment to measure humidity levels during calibrations and accounts for any changes that may occur when the gas flows through the inlet. The so-called “water ratio” is used hereon to represent humidity.

$$\text{water ratio} = \frac{\text{H}_2\text{OBr}^- (\text{cps})}{\text{Br}^- (\text{cps})} \quad (2)$$

I₂ calibrations were performed at a range of different humidities generated by changing the water mass supplied by the LCU. The range of I₂ concentrations for each humidity was between 1–3 x10¹⁰ molecules cm⁻³; about two orders of magnitude higher than what would typically be observed in the atmosphere. Ideally, the concentration range would be comparable to atmospheric levels, but limitations in the amount of gas dilution and water mass flow restricted the minimum concentrations that could be used. The I₂ sensitivity was determined by calculating the gradient of the calibration curves with units of ncps cm³ molecules⁻¹. The instrument response over the calibration range demonstrated a high degree of linearity, an example of which is shown in Fig. 3.

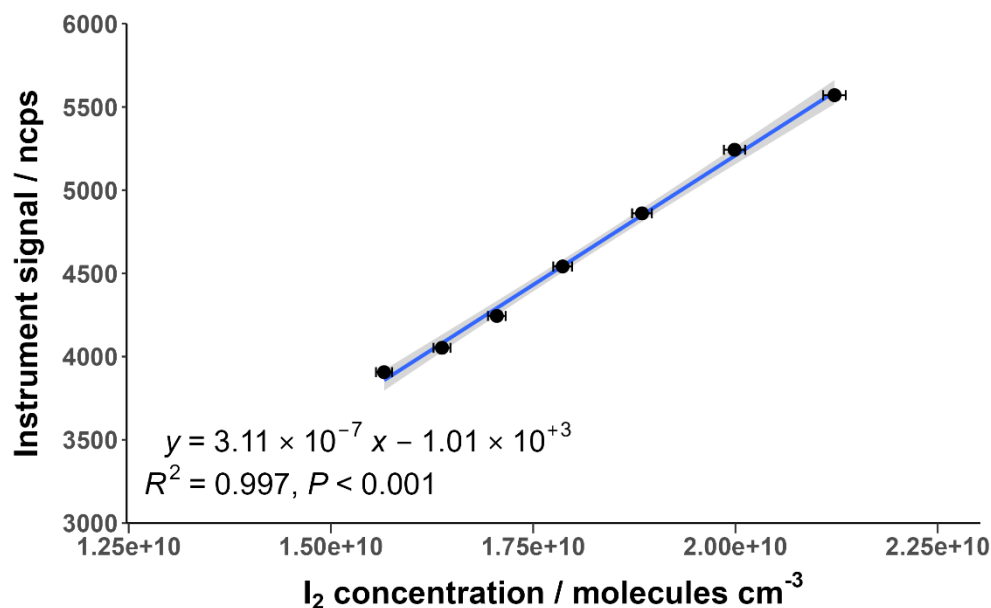


Figure 3: Normalised instrument signal against I_2 concentration for an example calibration at a water ratio of 1.05. The shaded area represents the 95% confidence interval of the fitted curve. Error bars indicate the calculated propagated uncertainty of the I_2 concentration, shown in section 3.5.

The change in I_2 sensitivity at different humidities is demonstrated in Fig 4. Above a water ratio of ~ 0.7 , the sensitivity of I_2 is effectively humidity-independent with a sensitivity of $3.25 \times 10^{-7} (\pm 6.30 \times 10^{-9})$ ncps cm^3 molecules $^{-1}$. This is four times more sensitive than the average sensitivity of $7.92 \times 10^{-8} (\pm 3.18 \times 10^{-9})$ ncps cm^3 molecules $^{-1}$ at near dryness (average water ratio = 0.0022), which can be attributed to the stabilising effect of the H_2O molecule on the formed adduct. At high humidities, this stabilising effect is balanced out by the lower formation enthalpy of adducts formed with the BrH_2O^+ reagent ion. There is also an increase in the formation of the second water cluster, $Br(H_2O)_2^+$, at very high humidities. There appears to be no literature on whether this cluster also acts as a reagent ion for I_2 . However, it is unlikely to act as one due to an additional collisional reaction needed for formation of $Br(H_2O)_2^+$ and the likely even lower formation enthalpy between the second water cluster and a sample molecule.

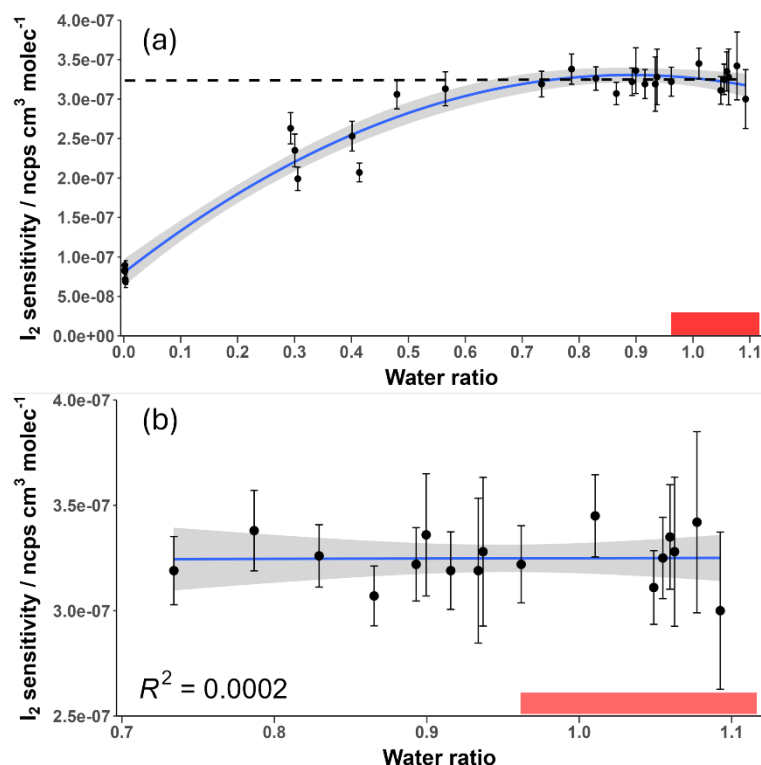


Figure 4: Measured I_2 sensitivity at different humidity levels over (a) the full range and (b) the humidity-independent range. Error bars represent the calculated error for each sensitivity value described in section 3.5. The shaded grey area represents the 95% confidence interval of the fitted curve. The shaded red region represents the ambient water ratio observed in the marine boundary layer at Tudor Hill, Bermuda. The dotted line in (a) is the average of the data points in (b).

3.4 HOI calibration and humidity dependence

The relative sensitivity of HOI compared to I_2 (termed the HOI/ I_2 ratio) was quantified by comparing the change in signal of HOI and I_2 with and without the NaI trap in place, with an example calibration shown in Fig. 5. With no trap in place, the ratio of HOI to I_2 signal was found to be around 1:5. On addition of the NaI trap, almost all of the HOI signal was removed with a corresponding increase in I_2 signal observed. For the equivalent HOBr–Br₂ system in the Liao et al. (2012) system, the conversion of HOBr to Br₂ was assumed to be 1:1. Here, the 1:1 HOI to I_2 conversion assumption was tested by measuring the signal of various other iodine-containing compounds, to determine whether any other significant reaction pathways were occurring during the production and destruction of HOI. The mass spectra of these other iodine compounds are shown without the NaI trap in Fig. A1 and including the trap in Fig. A2. On addition of the NaI trap, a small increase in signal was observed for HI and IBr. These quantities were much smaller than I_2 , which represented 96% of the change in signal. It is possible that the HI and IBr signal may be produced from HOI, for example if there was some NaBr also present in the trap. However, it is also possible that the presence of NaI is the cause of these compounds, such as any contaminant bromine compounds reacting



with NaI to produce IBr. Either way, the intensity of the signals for HI and IBr can be considered negligible and therefore substantiate the assumption of 1:1 conversion of HOI to I_2 .

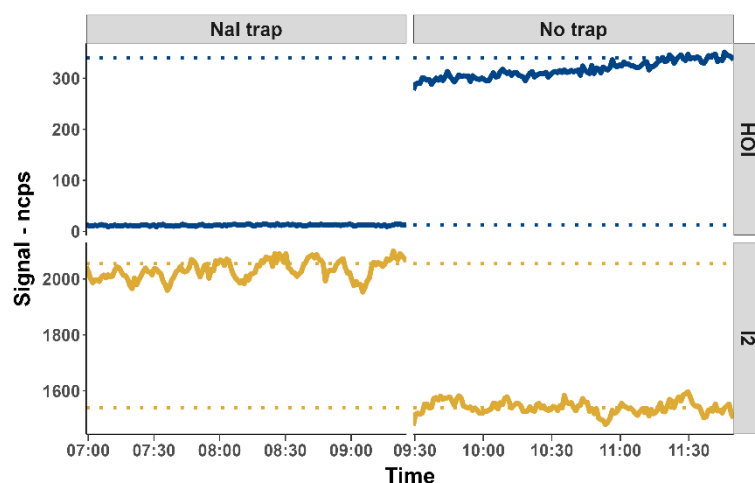


Figure 5: The 1-minute averaged HOI and I_2 normalised signal with and without the inclusion of the NaI trap. Dotted lines indicate the average signal of the final 20 minutes of each run.

The HOI calibration experiments were performed at different water ratios to determine how the HOI/ I_2 ratio changes with humidity. As water was required to generate HOI in the first stage of the calibration, the experiments were only able to be performed at relatively high humidity, between water ratios of 0.7 and 1.1. This range corresponds to the humidity-independent region found for I_2 . The humidity dependence of the HOI/ I_2 ratio is shown in Fig. 6.

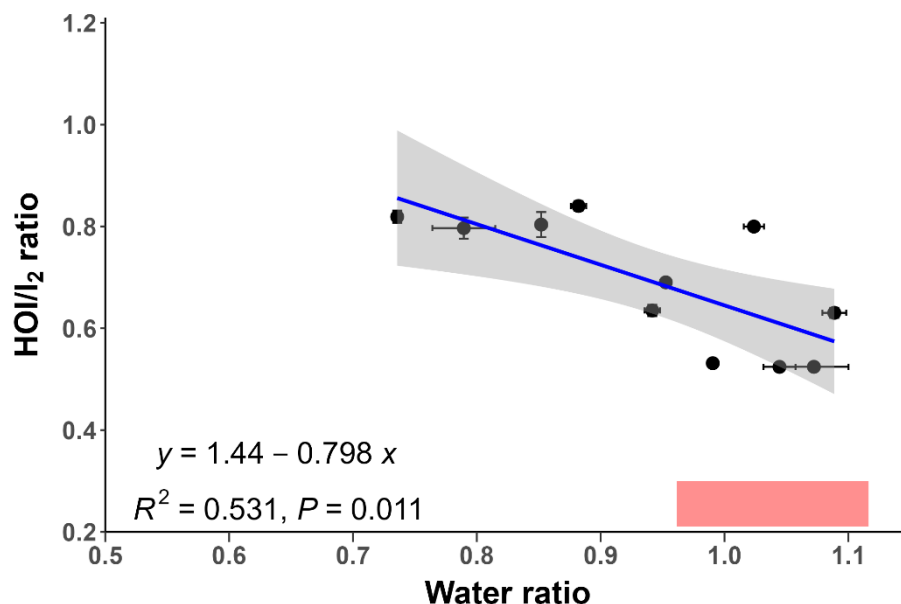


Figure 6: The relative sensitivity of HOI compared to I₂ (HOI/I₂ ratio) at different water ratio values. The shaded grey area represents the 95% confidence interval of the fitted regression line. The shaded red region represents the ambient water ratio observed in the marine boundary layer at Tudor Hill, Bermuda.

Figure 6 shows that the HOI/I₂ ratio moderately correlates with increasing humidity; the correlation is statistically significant with a P-value below 0.05. As the humidity dependence of I₂ is independent over this measurement range, this decrease is attributed to a decreasing sensitivity for HOI. This can be explained from a QRRK theory standpoint. The HOI.Br⁻ cluster has more harmonic oscillators than I₂.Br⁻, so the increase of harmonic oscillators from the presence of water has a smaller stabilising effect for HOI.Br⁻ than for I₂.Br⁻. Additionally, as the formation enthalpy for the HOI.Br⁻ cluster is lower than for I₂.Br⁻ (He et al., 2023), the effect of reducing the amount of dry cluster formation has a more pronounced effect on the HOI.Br⁻ cluster.

3.5 Sensitivity measurement uncertainty

Propagation of error was used to calculate the uncertainty of the I₂ and HOI sensitivities. This can be calculated using the exact formula of propagation, assuming that variables are independent of each other, as shown in Eq. (3).

$$\sigma_x = \sqrt{\left(\frac{\partial x}{\partial a}\right)^2 \cdot \sigma_a^2 + \left(\frac{\partial x}{\partial b}\right)^2 \cdot \sigma_b^2 + \left(\frac{\partial x}{\partial c}\right)^2 \cdot \sigma_c^2 + \dots + \left(\frac{\partial x}{\partial n}\right)^2 \cdot \sigma_n^2} \quad (3)$$

where a, b, c, \dots, n are the variables of the function x , ∂_x/∂_n is the partial derivative of the variable with respect to x , and σ_n is the error of the individual variable.



3.5.1 I₂

The I₂ concentration error was calculated from the propagation of the uncertainties of the emission of the I₂ permeation tube, the temperature of the permeation tube holder, and the total gas flow from the sample pump to give a relative error of 0.7%. The uncertainty of the sensitivity from a specific humidity calibration was calculated from the propagated uncertainty of the I₂ concentration and the instrument signal for each point in the calibration curve, as shown in Fig. 3. The uncertainties of the sensitivities in the humidity independent region can be averaged using Eq. (4) as these can be considered as repeats.

$$\sigma_{\text{humidity independent sensitivity}} = \frac{\sqrt{\sum_{i=1}^n (\sigma_i)^2}}{n} \quad (4)$$

where σ_i is the uncertainty of a particular sensitivity measurement and n is the number of measurements made in the humidity independent region.

This resulted in a sensitivity uncertainty of 6.30×10^{-9} ncps cm³ molecules⁻¹ for the humidity-independent region, corresponding to a relative error of 1.9%. This was repeated for the dry calibration sensitivities to produce an uncertainty of 3.18×10^{-9} ncps cm³ molecules⁻¹ which represents a relative error of 4.0%. This uncertainty encompasses both calibration and humidity-dependence uncertainties, but not background (zero) or inlet effects (see 3.6).

3.5.2 HOI

The sensitivity of HOI was determined relative to I₂ based on the linear model in Fig. 5. The uncertainty of the HOI sensitivity at a specific water ratio was found from the uncertainty of the I₂ sensitivity at that water ratio propagated with the uncertainty of the gradient and intercept of the linear model. This results in an uncertainty of 4.29×10^{-8} ncps cm³ molecules⁻¹ for the HOI sensitivity, corresponding to an average relative error of 19.8% with a range of 16-25%, neglecting any background and inlet effects.

3.6 Inlet loss considerations

Measuring gas-phase compounds through an instrument inlet will introduce gas-wall interactions that can lead to loss of signal or require conditioning to reach a steady state (Krechmer et al., 2016; Huang et al., 2018; Deming et al., 2019). Additionally, halogen compounds can undergo heterogeneous chemistry on inlet walls, resulting in conversion to other halogen compounds. This is particularly the case for the hypohalous acids and has been observed for HOBr and HOCl when measured by CIMS instruments (Neuman et al., 2010; Liao et al., 2014; Le Breton et al., 2017; Peng et al., 2022). While all halogen compounds experience these wall interactions, it is particularly pronounced for iodine compounds, leading to large losses and uncertainties in measurements. Previous measurements of I₂ have found sample line losses between 18–40% (Shaw and Carpenter, 2013; Carpenter et al., 2013). For HOI, the calibration performed by Tham et al. (2021) modelled the loss of HOI through their inlet system via diffusion to the inlet walls which contributed to their total HOI uncertainty of $\pm 55\%$.



The effect of inlet losses is heavily influenced by the instrument setup. This means that any differences in inlet configuration between calibrations and field measurements need to be accounted for. When deployed in the field, the inlet for this instrument had a PTFE guard, allowing sample air to enter the inlet at a 90° angle, shown in Fig. 7b. The guard was implemented with the intention that light gas-phase molecules could navigate around the bend without loss to the walls, but heavier aerosol particles could not, reducing the potential for aerosol to block the entrance to the CIMS instrument. However, when calibrating, the calibration gas was directed linearly into the sampling inlet, shown in Fig. 7a. The effect of this difference was investigated.

Two inlet loss experiments were performed, one using a PFA T-piece to investigate the effect of physically having a bend in place, and another with the PTFE guard that had been salted with sea water to mimic field conditions. A line of 1/8" PFA tubing was attached to the output of the HOI calibration system and held in two configurations: one where it is pushed past the bend as shown in Fig. 7c and one where it is held before it, Fig. 7d. This required altering the dilution flow to laboratory air to accommodate this configuration. The effect of the T-piece and PTFE guard on the normalised signal of HOI and I₂, along with other iodine compounds that are potentially present, are shown in Table 1.

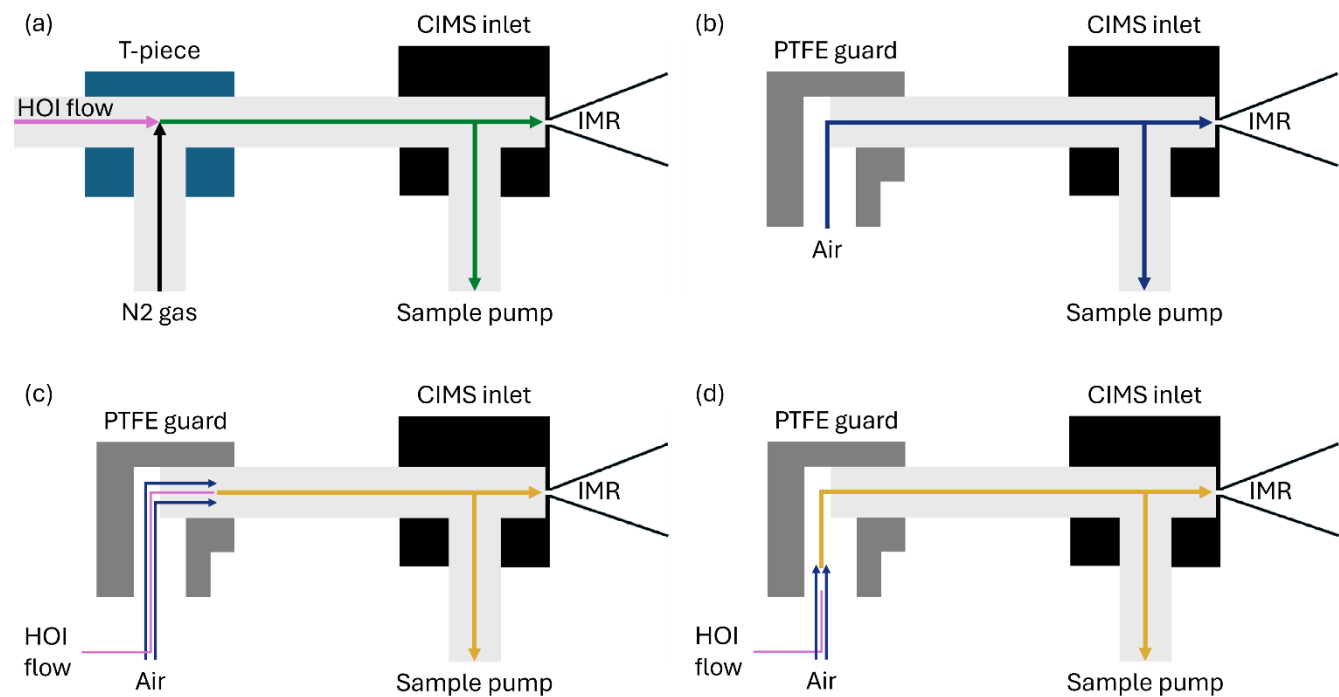


Figure 7: Simplified diagrams of the CIMS inlet setup during (a) the HOI calibration experiments, (b) sampling of air at Tudor Hill in Bermuda, (c) the line loss experiment bypassing the PTFE guard bend, (d) the line loss experiment including the bend from the PTFE guard.



Table 1: The normalised signal ± 1 standard deviation of various iodine species measured during the direct and bended inlet configurations for the T-piece and PTFE guard inlet loss experiments.

Species	T-piece			PTFE guard		
	Direct configuration $\pm 1\sigma$ / ncps	Bend configuration \pm 1σ / ncps	Signal difference / ncps (% change)	Direct configuration $\pm 1\sigma$	Bend configuration $\pm 1\sigma$	Signal difference / ncps (% change)
HOI	381.45 ± 5.85	132.79 ± 6.38	-248.66 (-65%)	335.05 ± 5.79	85.13 ± 2.59	-249.92 (-75%)
I ₂	2576.62 ± 25.92	2985.40 ± 49.75	+408.78 (+16%)	2149.51 ± 23.18	2472.60 ± 25.23	+323.09 (+15%)
ICl	371.44 ± 8.45	375.98 ± 10.53	+4.54 (+1%)	400.73 ± 8.62	531.58 ± 15.02	+130.85 (+33%)
IBr	20.82 ± 1.47	17.34 ± 1.81	-3.48 (-17%)	20.32 ± 1.51	185.06 ± 4.57	+164.74 (+811%)
HI	0.16 ± 0.42	0.20 ± 0.44	+0.04 (+25%)	0.17 ± 0.43	0.27 ± 0.47	+0.10 (+59%)
IO	1.04 ± 0.37	1.42 ± 0.71	+0.38 (+37%)	1.23 ± 0.35	1.02 ± 0.50	-0.21 (-17%)
HIO ₂	27.67 ± 3.77	30.36 ± 9.74	+2.69 (+10%)	26.73 ± 5.01	28.12 ± 4.75	+1.39 (+5%)
INO ₂	2.30 ± 0.73	1.00 ± 0.58	-1.30 (-57%)	2.36 ± 0.74	1.17 ± 0.50	-1.19 (-50%)
HIO ₃	0.79 ± 0.50	0.58 ± 0.64	-0.21 (-27%)	1.02 ± 0.56	0.93 ± 0.63	-0.09 (-9%)
IONO ₂	6.75 ± 1.39	2.51 ± 1.28	-4.24 (-63%)	6.48 ± 1.57	3.30 ± 1.33	-3.18 (-49%)



For both the T-piece and the guard, the direct signal is comparable in intensity to the signal seen during the HOI calibrations, with the exception of ICl, which is much higher than previously seen. When including the bend into the T-piece experiment, little variation in signal is observed for ICl, HI, IO, HIO₂, and HIO₃, with changes smaller than the standard deviation of the signal. There is a slight decrease in the IBr, INO₂, and IONO₂ signal, but the total quantity of loss from these compounds is small compared to the total loss (<4%). The most noticeable loss is observed with HOI, along with an accompanying increase in I₂. When converted into mixing ratios this corresponded to a 42.7 ppt (65%) HOI decrease and a 50.5 ppt (16%) increase in I₂. This conversion of HOI to I₂ likely proceeds via the reverse iodine hydrolysis reaction (R14). The I⁻ required is most likely from the HOI generation reaction in (R8), which becomes coated on the inlet walls. It is unknown how much I⁻ is present during field measurements, and so the observed I₂ increase found during the inlet loss tests may be an overestimate compared to atmospheric conditions.



With the salted PTFE guard, a higher proportion of HOI was lost (75% decrease) compared to the T-piece although the amount lost was similar at 43.4 ppt. Meanwhile the proportion of I₂ gain remained about the same (15% increase) but the amount has decreased to 40.0 ppt. There is a marked increase in IBr and ICl signal and the other iodine species remain at similar levels to the T-piece run. Cl⁻ and Br⁻ are abundant in sea salt aerosol and are known to react with HOI (Vogt et al., 1999; Braban et al., 2007; Tham et al., 2021), which is the likely reason for the increase in ICl and IBr and further loss of HOI compared to the T-piece experiment. The sensitivities for ICl and IBr have not been measured for Br-CIMS instruments. However, it has been suggested that sensitivities should be similar to that of I₂ (Wang et al., 2021a). If it is assumed that ICl and IBr have the same response to humidity as I₂, the signal change would correspond to a 16.9 and 20.2 ppt increase, respectively. This is far higher than would be expected from the additional HOI loss and may suggest there are additional pathways present to produce ICl and IBr. This again could be from the I⁻ present from the HOI production step though this likely requires oxidation before reacting with Cl⁻ and Br⁻.

3.7 Application to atmospheric HOI and I₂ data.

I₂ and HOI were measured by the Br-CIMS during the BLEACH campaign in June 2022 with the inlet configuration shown in Fig. 6b. Background signals were measured by flowing dry nitrogen (N₂) through a zero port in the CIMS inlet and through the instrument critical orifice to the IMR, with the rest of the sampled air directed through the sample pump. These zero measurements were repeated hourly, and the signal was linearly interpolated between measurements, providing a value for the background signal during sampling periods. The limit of detection (LoD) for I₂ and HOI were calculated from an extended zeroing period during the campaign as 3 standard deviations of the Allen variance of the zeroing period, similarly to that described in Riva et al. (2024). These corresponded to detection limits of 0.14 ppt for I₂ and 0.27 ppt for HOI.



The HOI calibration could not be performed at dryness, making zero subtraction difficult to quantify. It was expected that any signal observed in the zero was due to instrument noise rather than any interferent HOI. This was tested by comparing the relative signal intensities of two major isotope peaks of the HOI.Br⁻ adduct. The theoretical ratio between HOI.⁷⁹Br⁻ and HOI.⁸¹Br⁻ is 1:0.977 and so the zero data was tested to see whether the ratio between the two isotope peaks were within 10, 20 or 30% of this ratio or whether it fell outside these limits. These values are shown in Table 2. In total, 76% of the zero data had isotope ratios that were greater than the 30% tolerance, and so it was decided to not background subtract the HOI data. Therefore, the HOI data shown should be considered as an upper limit.

Table 2: The instrument zero data points during the BLEACH campaign that fell within various limits of the theoretical isotope ratio between the HOI.⁷⁹Br⁻ and HOI.⁸¹Br⁻ adduct signals. A ratio value that was greater than 30% of the theoretical value was considered to be outside the ratio tolerance.

	Total data points	Ratio limits			
		<10%	<20%	<30%	>30%
Zeroing data	242	16	33	58	184
	(100%)	(6.6%)	(13.6%)	(24.0%)	(76.0%)

Measured signals were converted into mixing ratios using the calibrations from Sect. 3.3 and 3.4 and applying the loss corrections described in Sect 3.5. The I₂ data was then zero subtracted using the linearly interpolated instrument zeros. Figure 8 shows the loss-corrected timeseries and diurnal cycles for I₂ and HOI. After zero subtractions and loss corrections, I₂ was detected between 0–0.7 ppt with some mixing ratios dropping to negative values. HOI ranged from 0.5–3.9 ppt after its loss corrections. There was little pattern in the diurnal cycle for I₂ with the average signal being between 0.1–0.3 ppt during both the day and night. The observed mixing ratios of I₂ are similar to previous open ocean measurements at the Cape Verde Atmospheric Observatory of <0.02–0.6 and <0.03–1.67 ppt in May 2007 and 2009 respectively (Lawler et al., 2014). These previous measurements observed a diurnal cycle for I₂ peaking at night, as expected due to its rapid photolysis. A diurnal cycle was not observed in our data, indicating either inlet or background effects which were not adequately quantified by our experiments or an unknown daytime source of I₂. The overall uncertainty of the I₂ measurements made during the BLEACH campaign, as seen in Sect. 3.7.1, and the fact that they were near to the detection limit of 0.14 ppt means that caution should be applied in interpreting the data.

A regular diurnal pattern was observed for HOI, with the signal consistently around 1 ppt during the night and increasing during the day to an average peak of around 2.75 ppt. There are no reported mixing ratios of HOI in the open ocean to compare to these values. The closest comparison is to the measurement of HOI at the coastal site of Mace Head (Tham et al., 2021). There, a diurnal cycle was also observed, with low nighttime mixing ratios and an increase during the day. However, the



amounts seen at Mace Head during the day were much higher (up to 66.6 ppt), likely due to photochemical reactions caused by I_2 emission by macroalgae (Tham et al., 2021).

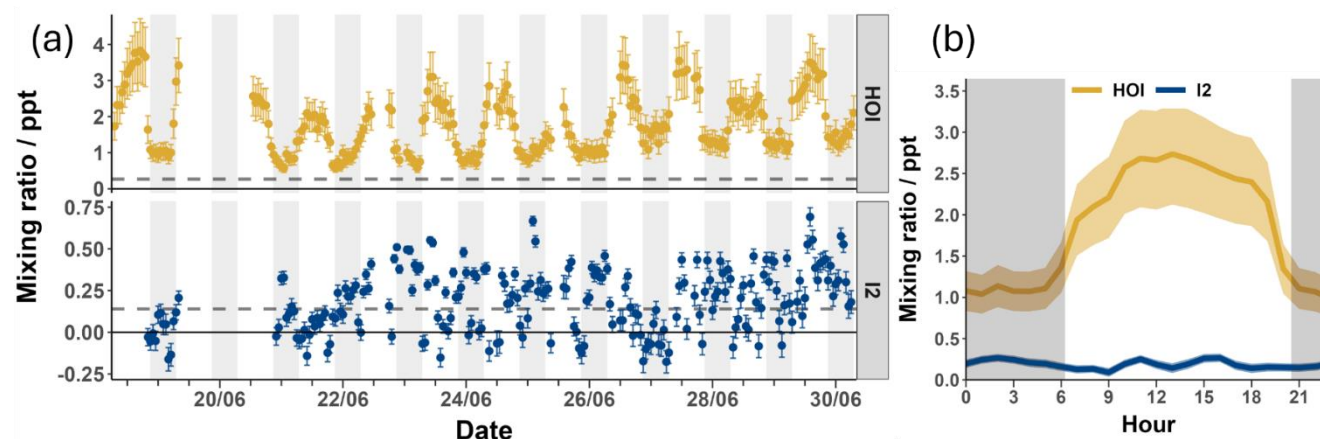


Figure 8: The timeseries (a) and diurnal cycle (b) of the mixing ratios of I_2 (blue) and HOI (yellow) from the BLEACH campaign in June 2022 after zero subtraction (for I_2) and loss correction (for both). The dashed line indicates the limit of detection for each compound. The average relative uncertainty of I_2 was $\pm 29.6\%$ and for HOI was $\pm 26.2\%$

3.7.1 Measurement uncertainties of atmospheric data

The uncertainty of the I_2 and HOI mixing ratios were again calculated by propagation of uncertainty. For I_2 , this was calculated from the uncertainty of the humidity independent sensitivity, twice the uncertainty of the dry sensitivity from the linear interpolation calculation, and the uncertainty of the instrument signal during the inlet loss experiment. This resulted in an average relative error throughout the BLEACH campaign of 29.6%. There are a number of other uncertainties from the inlet loss experiment that cannot be quantified and so the uncertainty for I_2 should be considered a lower limit. In future work, repeated experiments may be able to account for these uncertainties by finding a standard deviation of the loss correction value. The uncertainty of HOI was calculated with just the uncertainty from the humidity dependent sensitivity and the uncertainty of the instrument signal during the inlet loss experiment, resulting in an average relative error of 26.2% throughout the BLEACH campaign. The HOI uncertainty value should also be considered a lower limit as there are the other unquantified uncertainties of the inlet loss experiment and a lack of a zero subtraction.

4. Summary and conclusions

There have been few atmospheric measurements of HOI and I_2 due to the requirement of highly sensitive and selective instrumentation and the lack of readily available calibration methods for HOI. In this study, we demonstrate a novel method for the generation and calibration of HOI at ppt levels, utilising its interconversion to I_2 via chemical traps. The presence of potential interferent iodine compounds was found to be negligible and the calibration was shown to be repeatable over a range of humidities. The developed calibration method was utilised to ascertain the humidity dependence of the CIMS for HOI and



I₂. It was found that at humidities typical of the marine boundary layer, I₂ exhibited a humidity-independent sensitivity whereas HOI showed a slight negative dependency. A possible explanation, supported by QRRK theory, is that higher humidities increase the proportion of the Br(H₂O)⁻ reagent ion, which has a lower adduct formation enthalpy with HOI and I₂ compared to the Br⁻ reagent ion, resulting in decreased sensitivities. However, the presence of H₂O increases the available harmonic oscillators of the adduct, improving the energy distribution and stabilisation of the adduct and increasing its sensitivity. This effect is greater for I₂.Br⁻ as it has fewer harmonic oscillators than HOI.Br⁻ and these two opposing factors mean that the sensitivity of I₂.Br⁻ is humidity independent. However, this stabilisation is not sufficient in the case of the HOI.Br⁻ adduct to mitigate the increasing proportion of Br(H₂O)⁻ vs Br⁻ reagent ions, resulting in a decreased sensitivity at high humidities.

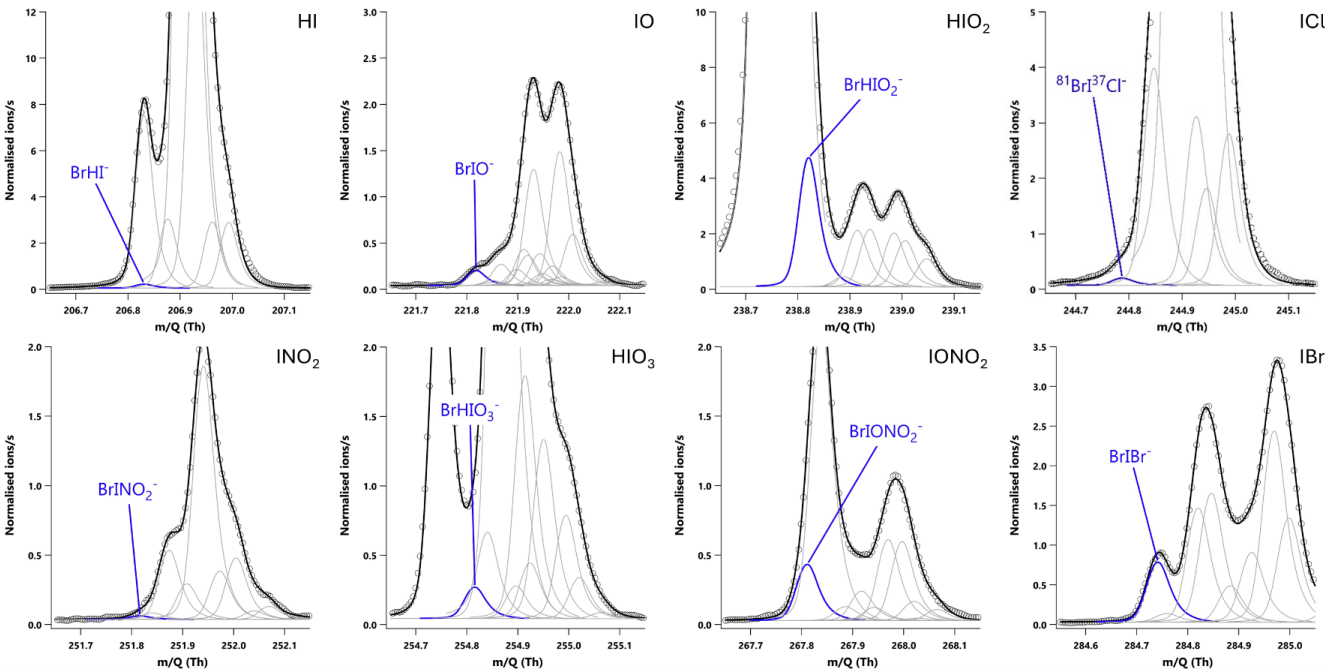
Heterogeneous chemistry and inlet wall losses are a perennial problem in the measurement of acidic and reactive species, which can be exacerbated depending on the inlet configuration. When using the inlet configuration made for field measurements, up to 75% of the HOI signal was lost compared to the calibration setup. This was accompanied by a corresponding increase in I₂ signal, suggesting that this loss occurred via the reverse hydrolysis of iodine.

After correcting for humidity sensitivities and inlet losses, we detected I₂ and HOI in the marine boundary layer during the BLEACH campaign at Tudor Hill, Bermuda in June 2022 at mixing ratios of between 0–0.7 ppt for I₂ and an upper limit of 0.5–3.8 ppt for HOI. The overall uncertainty of these measurements was calculated as ± 29.6% for I₂ and ± 26.3% for HOI. These uncertainties can be considered as lower limits as there were additional uncertainties from the inlet loss experiment that were not quantifiable. Additionally, zero subtraction could not be performed for the HOI data which could further increase the relative error.

In future work, the accuracy for I₂ and HOI could be improved by performing background measurements at similar humidity levels to the ambient measurements, reducing the need to account for large differences in sensitivities from different humidities. Additionally, further work on the HOI calibration can further constrain the uncertainty of the humidity dependent HOI/I₂ ratio over a wider range of humidities. Finally, development of atmospheric detection of HOI and I₂ should focus on using instrument inlets that can minimise inlet effects for these compounds, reducing the need to perform correction tests.



482 **Appendix**



483 **Figure A1: 20-minute averaged high resolution single peak mass spectra fits for potential iodine containing compounds during the**
484 **HOI calibrations with the NaI trap in place.**
485

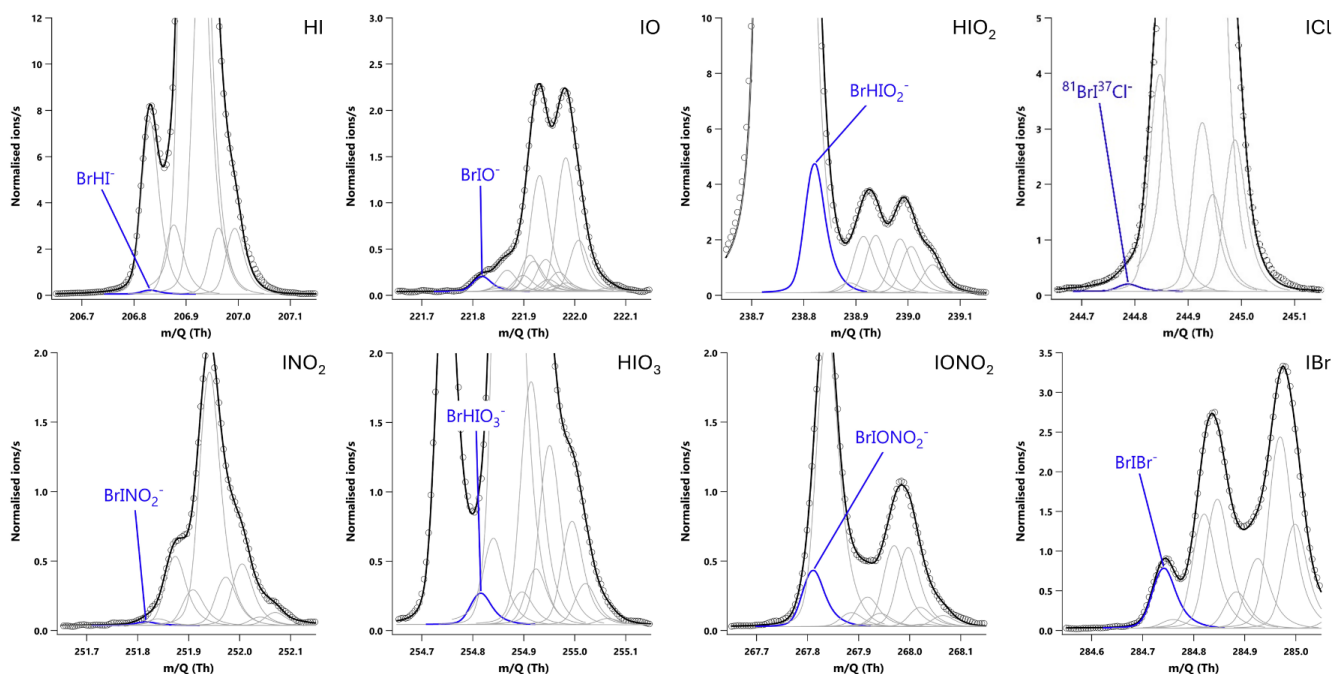


Figure A2: 20-minute averaged high resolution single peak mass spectra fits for potential iodine containing compounds during the HOI calibrations after the removal of the NaI trap.



490 **Data availability**

491 Datasets for the figures shown are available at: <https://doi.org/10.15124/48ade8f3-d750-4fe6-a2d9-b8f69bf86262>

492 **Author contribution**

493 LM, MS, LJC and SJA designed and developed the humidity dependence calibrations for I₂ which were conducted by LM.
494 MS, PR and JT developed the HOI calibration method and was adapted and conducted in lab experiments by LM and MZ.
495 BA was responsible for the management and coordination of the BLEACH field campaign and AP was responsible for the
496 management and usage of the Tudor Hill Marine Atmospheric Observatory.
497 LM and LJC prepared the paper, and all authors reviewed the paper.

498 **Competing interests**

499 The authors declare that they have no conflict of interest.

500 **Acknowledgements**

501 The authors would like to thank John Halfacre, William Drysdale, Allison Moon, Alyson Fritzmann and Gordon Novak for
502 their help during the BLEACH summer campaign.

503 **Financial support**

504 This research was supported by the European Research Council, Horizon Europe European Research Council (grant no.
505 833290).
506 BA, JT and PR were supported by NSF AGS 2109323
507 The Tudor Hill Marine Atmospheric Observatory was supported by the National Science Foundation's Chemical
508 Oceanography Program, grant OCE-2123053.

509 **References**

510 Auzmendi-Murua, I., Castillo, A., and Bozzelli, J.: Mercury Oxidation via Chlorine, Bromine, and Iodine under Atmospheric
511 Conditions: Thermochemistry and Kinetics, JOURNAL OF PHYSICAL CHEMISTRY A, 118, 2959-2975,
512 10.1021/jp412654s, 2014.
513 Bitter, M., Ball, S., Povey, I., and Jones, R.: A broadband cavity ringdown spectrometer for in-situ measurements of
514 atmospheric trace gases, ATMOSPHERIC CHEMISTRY AND PHYSICS, 5, 2547-2560, 2005.



- 515 Breitenlechner, M., Novak, G., Neuman, J., Rollins, A., and Veres, P.: A versatile vacuum ultraviolet ion source for reduced
516 pressure bipolar chemical ionization mass spectrometry, *ATMOSPHERIC MEASUREMENT TECHNIQUES*, 15, 1159-1169,
517 10.5194/amt-15-1159-2022, 2022.
- 518 Buys, Z., Brough, N., Huey, L., Tanner, D., von Glasow, R., and Jones, A.: High temporal resolution Br₂, BrCl and BrO
519 observations in coastal Antarctica, *ATMOSPHERIC CHEMISTRY AND PHYSICS*, 13, 1329-1343, 10.5194/acp-13-1329-
520 2013, 2013.
- 521 Calvert, J. G. and Lindberg, S. E.: The potential influence of iodine-containing compounds on the chemistry of the troposphere
522 in the polar spring. II. Mercury depletion, *Atmospheric Environment*, 38, 5105-5116, 10.1016/j.atmosenv.2004.05.050, 2004.
- 523 Caram, C., Szopa, S., Cozic, A., Bekki, S., Cuevas, C., and Saiz-Lopez, A.: Sensitivity of tropospheric ozone to halogen
524 chemistry in the chemistry-climate model LMDZ-INCA vNMHC, *GEOSCIENTIFIC MODEL DEVELOPMENT*, 16, 4041-
525 4062, 10.5194/gmd-16-4041-2023, 2023.
- 526 Carpenter, L. J., MacDonald, S. M., Shaw, M. D., Kumar, R., Saunders, R. W., Parthipan, R., Wilson, J., and Plane, J. M. C.:
527 Atmospheric iodine levels influenced by sea surface emissions of inorganic iodine, *Nature Geoscience*, 6, 108-111,
528 10.1038/ngeo1687, 2013.
- 529 Chameides, W. L. and Davis, D. D.: IODINE - ITS POSSIBLE ROLE IN TROPOSPHERIC PHOTOCHEMISTRY, *Journal*
530 *of Geophysical Research-Oceans*, 85, 7383-7398, 10.1029/JC085iC12p07383, 1980.
- 531 Cuevas, C. A., Maffezzoli, N., Corella, J. P., Spolaor, A., Vallenga, P., Kjaer, H. A., Simonsen, M., Winstrup, M., Vinther,
532 B., Horvat, C., Fernandez, R. P., Kinnison, D., Lamarque, J. F., Barbante, C., and Saiz-Lopez, A.: Rapid increase in
533 atmospheric iodine levels in the North Atlantic since the mid-20th century, *Nature Communications*, 9, 6, 10.1038/s41467-
534 018-03756-1, 2018.
- 535 Custard, K., Pratt, K., Wang, S., and Shepson, P.: Constraints on Arctic Atmospheric Chlorine Production through
536 Measurements and Simulations of Cl₂ and ClO, *ENVIRONMENTAL SCIENCE & TECHNOLOGY*, 50, 12394-
537 12400, 10.1021/acs.est.6b03909, 2016.
- 538 Deming, B., Pagonis, D., Liu, X., Day, D., Talukdar, R., Krechmer, J., de Gouw, J., Jimenez, J., and Ziemann, P.:
539 Measurements of delays of gas-phase compounds in a wide variety of tubing materials due to gas-wall interactions,
540 *ATMOSPHERIC MEASUREMENT TECHNIQUES*, 12, 3453-3461, 10.5194/amt-12-3453-2019, 2019.
- 541 Dörich, R., Eger, P., Lelieveld, J., and Crowley, J.: Iodide CIMS and m/z 62: the detection of HNO₃ as NO₃- in the presence
542 of PAN, peroxyacetic acid and ozone, *ATMOSPHERIC MEASUREMENT TECHNIQUES*, 14, 5319-5332, 10.5194/amt-14-
543 5319-2021, 2021.
- 544 Finkenzeller, H., Iyer, S., He, X., Simon, M., Koenig, T., Lee, C., Valiev, R., Hofbauer, V., Amorim, A., Baalbaki, R.,
545 Baccarini, A., Beck, L., Bell, D., Caudillo, L., Chen, D., Chiu, R., Chu, B., Dada, L., Duplissy, J., ..., and Volkamer, R.: The
546 gas-phase formation mechanism of iodic acid as an atmospheric aerosol source, *NATURE CHEMISTRY*, 15, 129-+,
547 10.1038/s41557-022-01067-z, 2023.
- 548 Garland, J. A., Elzerman, A. W., and Penkett, S. A.: THE MECHANISM FOR DRY DEPOSITION OF OZONE TO
549 SEAWATER SURFACES, *Journal of Geophysical Research-Oceans*, 85, 7488-7492, 10.1029/JC085iC12p07488, 1980.
- 550 He, X., Shen, J., Iyer, S., Juuti, P., Zhang, J., Koirala, M., Kytökari, M., Worsnop, D., Rissanen, M., Kulmala, M., Maier, N.,
551 Mikkilä, J., Sipilä, M., and Kangasluoma, J.: Characterisation of gaseous iodine species detection using the multi-scheme
552 chemical ionisation inlet 2 with bromide and nitrate chemical ionisation methods, *ATMOSPHERIC MEASUREMENT*
553 *TECHNIQUES*, 16, 4461-4487, 10.5194/amt-16-4461-2023, 2023.
- 554 Huang, R., Seitz, K., Buxmann, J., Pöhler, D., Hornsby, K., Carpenter, L., Platt, U., and Hoffmann, T.: In situ measurements
555 of molecular iodine in the marine boundary layer: the link to macroalgae and the implications for O₃, IO, OIO
556 and NO_x, *ATMOSPHERIC CHEMISTRY AND PHYSICS*, 10, 4823-4833, 10.5194/acp-10-4823-2010, 2010.
- 557 Huang, Y., Zhao, R., Charan, S., Kenseth, C., Zhang, X., and Seinfeld, J.: Unified Theory of Vapor-Wall Mass Transport in
558 Teflon-Walled Environmental Chambers, *ENVIRONMENTAL SCIENCE & TECHNOLOGY*, 52, 2134-2142,
559 10.1021/acs.est.7b05575, 2018.
- 560 Huey, L.: Measurement of trace atmospheric species by chemical ionization mass spectrometry: Speciation of reactive nitrogen
561 and future directions, *MASS SPECTROMETRY REVIEWS*, 26, 166-184, 10.1002/mas.20118, 2007.
- 562 Iglesias-Suarez, F., Badia, A., Fernandez, R. P., Cuevas, C. A., Kinnison, D. E., Tilmes, S., Lamarque, J. F., Long, M. C.,
563 Hossaini, R., and Saiz-Lopez, A.: Natural halogens buffer tropospheric ozone in a changing climate, *Nature Climate Change*,
564 10, 147-+, 10.1038/s41558-019-0675-6, 2020.



Iyer, S., Lopez-Hilfiker, F., Lee, B., Thornton, J., and Kurtén, T.: Modeling the Detection of Organic and Inorganic Compounds Using Iodide-Based Chemical Ionization, *JOURNAL OF PHYSICAL CHEMISTRY A*, 120, 576-587, 10.1021/acs.jpca.5b09837, 2016.

Ji, Y., Huey, G., Tanner, D. J., Lee, Y. R., Veres, P. R., Neuman, J. A., Wang, Y. H., and Wang, X. M.: A vacuum ultraviolet ion source (VUV-IS) for iodide-chemical ionization mass spectrometry: a substitute for radioactive ion sources, *Atmospheric Measurement Techniques*, 13, 3683-3696, 10.5194/amt-13-3683-2020, 2020.

Kassel, L. S.: Studies in homogeneous gas reactions II Introduction of quantum theory, *Journal of Physical Chemistry*, 32, 1065-1079, 10.1021/j150289a011, 1928.

Kercher, J. P., Riedel, T. P., and Thornton, J. A.: Chlorine activation by N_2O_5 : simultaneous, in situ detection of ClNO_2 and N_2O_5 by chemical ionization mass spectrometry, *Atmospheric Measurement Techniques*, 2, 193-204, 10.5194/amt-2-193-2009, 2009.

Klobas, J., Hansen, J., Weisenstein, D., Kennedy, R., and Wilmouth, D.: Sensitivity of Iodine-Mediated Stratospheric Ozone Loss Chemistry to Future Chemistry-Climate Scenarios, *FRONTIERS IN EARTH SCIENCE*, 9, 10.3389/feart.2021.617586, 2021.

Koenig, T., Baidar, S., Campuzano-Jost, P., Cuevas, C., Dix, B., Fernandez, R., Guo, H., Hall, S., Kinnison, D., Nault, B., Ullmann, K., Jimenez, J., Saiz-Lopez, A., and Volkamer, R.: Quantitative detection of iodine in the stratosphere, *PROCEEDINGS OF THE NATIONAL ACADEMY OF SCIENCES OF THE UNITED STATES OF AMERICA*, 117, 1860-1866, 10.1073/pnas.1916828117, 2020.

Krechmer, J., Pagonis, D., Ziemann, P., and Jimenez, J.: Quantification of Gas-Wall Partitioning in Teflon Environmental Chambers Using Rapid Bursts of Low-Volatility Oxidized Species Generated in Situ, *ENVIRONMENTAL SCIENCE & TECHNOLOGY*, 50, 5757-5765, 10.1021/acs.est.6b00606, 2016.

Kurtén, T., Kuang, C. A., Gómez, P., McMurtry, P. H., Vehkamäki, H., Ortega, I., Noppel, M., and Kulmala, M.: The role of cluster energy nonaccommodation in atmospheric sulfuric acid nucleation, *Journal of Chemical Physics*, 132, 8, 10.1063/1.3291213, 2010.

Lawler, M., Mahajan, A., Saiz-Lopez, A., and Saltzman, E.: Observations of I_2 at a remote marine site, *ATMOSPHERIC CHEMISTRY AND PHYSICS*, 14, 2669-2678, 10.5194/acp-14-2669-2014, 2014.

Lawler, M. J., Sander, R., Carpenter, L. J., Lee, J. D., Von Glasow, R., Sommariva, R., and Saltzman, E. S.: HOCl and Cl_2 observations in marine air, *Atmospheric Chemistry and Physics*, 11, 7617-7628, 10.5194/acp-11-7617-2011, 2011.

Le Breton, M., Bannan, T., Shallcross, D., Khan, M., Evans, M., Lee, J., Lidster, R., Andrews, S., Carpenter, L., Schmidt, J., Jacob, D., Harris, N., Bauguutte, S., Gallagher, M., Bacak, A., Leather, K., and Percival, C.: Enhanced ozone loss by active inorganic bromine chemistry in the tropical troposphere, *ATMOSPHERIC ENVIRONMENT*, 155, 21-28, 10.1016/j.atmosenv.2017.02.003, 2017.

Lee, B., Lopez-Hilfiker, F., Veres, P., McDuffie, E., Fibiger, D., Sparks, T., Ebben, C., Green, J., Schroder, J., Campuzano-Jost, P., Iyer, S., D'Ambro, E., Schobesberger, S., Brown, S., Wooldridge, P., Cohen, R., Fiddler, M., Bililign, S., Jimenez, J., ..., and Thornton, J.: Flight Deployment of a High-Resolution Time-of-Flight Chemical Ionization Mass Spectrometer: Observations of Reactive Halogen and Nitrogen Oxide Species, *JOURNAL OF GEOPHYSICAL RESEARCH-ATMOSPHERES*, 123, 7670-7686, 10.1029/2017JD028082, 2018.

Lee, B. H., Lopez-Hilfiker, F. D., Mohr, C., Kurtén, T., Worsnop, D. R., and Thornton, J. A.: An Iodide-Adduct High-Resolution Time-of-Flight Chemical-Ionization Mass Spectrometer: Application to Atmospheric Inorganic and Organic Compounds, *Environmental Science & Technology*, 48, 6309-6317, 10.1021/es500362a, 2014.

Lee, C., Elgiar, T., David, L., Wilmot, T., Reza, M., Hirshorn, N., McCubbin, I., Shah, V., Lin, J., Lyman, S., Hallar, A., Gratz, L., and Volkamer, R.: Elevated Tropospheric Iodine Over the Central Continental United States: Is Iodine a Major Oxidant of Atmospheric Mercury?, *GEOPHYSICAL RESEARCH LETTERS*, 51, 10.1029/2024GL109247, 2024.

Legrand, M., McConnell, J., Preunkert, S., Arienzo, M., Chellman, N., Gleason, K., Sherwen, T., Evans, M., and Carpenter, L.: Alpine ice evidence of a three-fold increase in atmospheric iodine deposition since 1950 in Europe due to increasing oceanic emissions, *PROCEEDINGS OF THE NATIONAL ACADEMY OF SCIENCES OF THE UNITED STATES OF AMERICA*, 115, 12136-12141, 10.1073/pnas.1809867115, 2018.



Liao, J., Huey, L., Liu, Z., Tanner, D., Cantrell, C., Orlando, J., Flocke, F., Shepson, P., Weinheimer, A., Hall, S., Ullmann, K., Beine, H., Wang, Y., Ingall, E., Stephens, C., Hornbrook, R., Apel, E., Riemer, D., Fried, A., ..., and Nowak, J.: High levels of molecular chlorine in the Arctic atmosphere, *NATURE GEOSCIENCE*, 7, 91-94, 10.1038/NGEO2046, 2014.

Liao, J., Huey, L. G., Scheuer, E., Dibb, J. E., Stickel, R. E., Tanner, D. J., Neuman, J. A., Nowak, J. B., Choi, S., Wang, Y., Salawitch, R. J., Canty, T., Chance, K., Kurosu, T., Suleiman, R., Weinheimer, A. J., Shetter, R. E., Fried, A., Brune, W., ..., and Ingall, E. D.: Characterization of soluble bromide measurements and a case study of BrO observations during ARCTAS, *Atmospheric Chemistry and Physics*, 12, 1327-1338, 10.5194/acp-12-1327-2012, 2012.

MacDonald, S., Martín, J., Chance, R., Warriner, S., Saiz-Lopez, A., Carpenter, L., and Plane, J.: A laboratory characterisation of inorganic iodine emissions from the sea surface: dependence on oceanic variables and parameterisation for global modelling, *ATMOSPHERIC CHEMISTRY AND PHYSICS*, 14, 5841-5852, 10.5194/acp-14-5841-2014, 2014.

Mahajan, A., Oetjen, H., Saiz-Lopez, A., Lee, J., McFiggans, G., and Plane, J.: Reactive iodine species in a semi-polluted environment, *GEOPHYSICAL RESEARCH LETTERS*, 36, 10.1029/2009GL038018, 2009.

Marcy, T., Gao, R., Northway, M., Popp, P., Stark, H., and Fahey, D.: Using chemical ionization mass spectrometry for detection of HNO₃, HOI, and ClONO₂ in the atmosphere, *INTERNATIONAL JOURNAL OF MASS SPECTROMETRY*, 243, 63-70, 10.1016/j.ijms.2004.11.012, 2005.

Neale, P., Hylander, S., Banaszak, A., Häder, D., Rose, K., Vione, D., Wängberg, S., Jansen, M., Busquets, R., Andersen, M., Madronich, S., Hanson, M., Schikowski, T., Solomon, K., Sulzberger, B., Wallington, T., Heikkilä, A., Pandey, K., Andradý, A., ..., and Zepp, R.: Environmental consequences of interacting effects of changes in stratospheric ozone, ultraviolet radiation, and climate: UNEP Environmental Effects Assessment Panel, Update 2024, *PHOTOCHEMICAL & PHOTOBIOLOGICAL SCIENCES*, 24, 357-392, 10.1007/s43630-025-00687-x, 2025.

Neuman, J., Nowak, J., Huey, L., Burkholder, J., Dibb, J., Holloway, J., Liao, J., Peischl, J., Roberts, J., Ryerson, T., Scheuer, E., Stark, H., Stickel, R., Tanner, D., and Weinheimer, A.: Bromine measurements in ozone depleted air over the Arctic Ocean, *ATMOSPHERIC CHEMISTRY AND PHYSICS*, 10, 6503-6514, 10.5194/acp-10-6503-2010, 2010.

O'Dowd, C., Hämeri, K., Mäkelä, J., Väkeva, M., Aalto, P., de Leeuw, G., Kunz, G., Becker, E., Hansson, H., Allen, A., Harrison, R., Berresheim, H., Geever, M., Jennings, S., and Kulmala, M.: Coastal new particle formation:: Environmental conditions and aerosol physicochemical characteristics during nucleation bursts -: art. no. 8107, *JOURNAL OF GEOPHYSICAL RESEARCH-ATMOSPHERES*, 107, 10.1029/2000JD000206, 2002.

Peng, X., Wang, T., Wang, W., Ravishankara, A., George, C., Xia, M., Cai, M., Li, Q., Salvador, C., Lau, C., Lyu, X., Poon, C., Mellouki, A., Mu, Y., Hallquist, M., Saiz-Lopez, A., Guo, H., Herrmann, H., Yu, C., ..., and Chen, J.: Photodissociation of particulate nitrate as a source of daytime tropospheric Cl₂, *NATURE COMMUNICATIONS*, 13, 10.1038/s41467-022-28383-9, 2022.

Peters, C., Pechtl, S., Stutz, J., Hebestreit, K., Hönninger, G., Heumann, K., Schwarz, A., Winterlik, J., and Platt, U.: Reactive and organic halogen species in three different European coastal environments, *ATMOSPHERIC CHEMISTRY AND PHYSICS*, 5, 3357-3375, 2005.

Pound, R., Durcan, D., Evans, M., and Carpenter, L.: Comparing the Importance of Iodine and Isoprene on Tropospheric Photochemistry, *GEOPHYSICAL RESEARCH LETTERS*, 50, 10.1029/2022GL100997, 2023.

Prados-Roman, C., Cuevas, C., Hay, T., Fernandez, R., Mahajan, A., Royer, S., Galí, M., Simó, R., Dachs, J., Grossmann, K., Kinnison, D., Lamarque, J., and Saiz-Lopez, A.: Iodine oxide in the global marine boundary layer, *ATMOSPHERIC CHEMISTRY AND PHYSICS*, 15, 583-593, 10.5194/acp-15-583-2015, 2015.

Priestley, M., le Breton, M., Bannan, T., Worrall, S., Bacak, A., Smedley, A., Reyes-Villegas, E., Mehra, A., Allan, J., Webb, A., Shallcross, D., Coe, H., and Percival, C.: Observations of organic and inorganic chlorinated compounds and their contribution to chlorine radical concentrations in an urban environment in northern Europe during the wintertime, *ATMOSPHERIC CHEMISTRY AND PHYSICS*, 18, 13481-13493, 10.5194/acp-18-13481-2018, 2018.

Read, K. A., Mahajan, A. S., Carpenter, L. J., Evans, M. J., Faria, B. V. E., Heard, D. E., Hopkins, J. R., Lee, J. D., Moller, S. J., Lewis, A. C., Mendes, L., McQuaid, J. B., Oetjen, H., Saiz-Lopez, A., Pilling, M. J., and Plane, J. M. C.: Extensive halogen-mediated ozone destruction over the tropical Atlantic Ocean, *Nature*, 453, 1232-1235, 10.1038/nature07035, 2008.

Rice, O. K. and Ramsperger, H. C.: Theories of unimolecular gas reactions at low pressures, *Journal of the American Chemical Society*, 49, 1617-1629, 10.1021/ja01406a001, 1927.



- Rissanen, M., Mikkilä, J., Iyer, S., and Hakala, J.: Multi-scheme chemical ionization inlet (MION) for fast switching of reagent ion chemistry in atmospheric pressure chemical ionization mass spectrometry (CIMS) applications, *ATMOSPHERIC MEASUREMENT TECHNIQUES*, 12, 6635-6646, 10.5194/amt-12-6635-2019, 2019.
- Riva, M., Pospisilova, V., Frege, C., Perrier, S., Bansal, P., Jorga, S., Sturm, P., Thornton, J., Rohner, U., and Lopez-Hilfiker, F.: Evaluation of a reduced-pressure chemical ion reactor utilizing adduct ionization for the detection of gaseous organic and inorganic species, *ATMOSPHERIC MEASUREMENT TECHNIQUES*, 17, 5887-5901, 10.5194/amt-17-5887-2024, 2024.
- Roscoe, H., Brough, N., Jones, A., Wittrock, F., Richter, A., Van Roozendaal, M., and Hendrick, F.: Characterisation of vertical BrO distribution during events of enhanced tropospheric BrO in Antarctica, from combined remote and in-situ measurements, *JOURNAL OF QUANTITATIVE SPECTROSCOPY & RADIATIVE TRANSFER*, 138, 70-81, 10.1016/j.jqsrt.2014.01.026, 2014.
- Saiz-Lopez, A. and Plane, J.: Novel iodine chemistry in the marine boundary layer, *GEOPHYSICAL RESEARCH LETTERS*, 31, 10.1029/2003GL019215, 2004.
- Saiz-Lopez, A. and von Glasow, R.: Reactive halogen chemistry in the troposphere, *CHEMICAL SOCIETY REVIEWS*, 41, 6448-6472, 10.1039/c2cs35208g, 2012.
- Saiz-Lopez, A., Fernandez, R. P., Ordonez, C., Kinnison, D. E., Martin, J. C. G., Lamarque, J. F., and Tilmes, S.: Iodine chemistry in the troposphere and its effect on ozone, *Atmospheric Chemistry and Physics*, 14, 13119-13143, 10.5194/acp-14-13119-2014, 2014.
- Saiz-Lopez, A., Plane, J. M. C., Baker, A. R., Carpenter, L. J., von Glasow, R., Martin, J. C. G., McFiggans, G., and Saunders, R. W.: Atmospheric Chemistry of Iodine, *Chemical Reviews*, 112, 1773-1804, 10.1021/cr200029u, 2012.
- Sanchez, J., Tanner, D., Chen, D., Huey, L., and Ng, N.: A new technique for the direct detection of HO₂ radicals using bromide chemical ionization mass spectrometry (Br-CIMS): initial characterization, *ATMOSPHERIC MEASUREMENT TECHNIQUES*, 9, 3851-3861, 10.5194/amt-9-3851-2016, 2016.
- Shaw, M. and Carpenter, L.: Modification of Ozone Deposition and I₂ Emissions at the Air-Aqueous Interface by Dissolved Organic Carbon of Marine Origin, *ENVIRONMENTAL SCIENCE & TECHNOLOGY*, 47, 10947-10954, 10.1021/es4011459, 2013.
- Sherwen, T., Evans, M. J., Carpenter, L. J., Andrews, S. J., Lidster, R. T., Dix, B., Koenig, T. K., Sinreich, R., Ortega, I., Volkamer, R., Saiz-Lopez, A., Prados-Roman, C., Mahajan, A. S., and Ordonez, C.: Iodine's impact on tropospheric oxidants: a global model study in GEOS-Chem, *Atmospheric Chemistry and Physics*, 16, 1161-1186, 10.5194/acp-16-1161-2016, 2016a.
- Sherwen, T., Schmidt, J., Evans, M., Carpenter, L., Grossmann, K., Eastham, S., Jacob, D., Dix, B., Koenig, T., Sinreich, R., Ortega, I., Volkamer, R., Saiz-Lopez, A., Prados-Roman, C., Mahajan, A., and Ordóñez, C.: Global impacts of tropospheric halogens (Cl, Br, I) on oxidants and composition in GEOS-Chem, *ATMOSPHERIC CHEMISTRY AND PHYSICS*, 16, 12239-12271, 10.5194/acp-16-12239-2016, 2016b.
- Simpson, W. R., Brown, S. S., Saiz-Lopez, A., Thornton, J. A., and von Glasow, R.: Tropospheric Halogen Chemistry: Sources, Cycling, and Impacts, *Chemical Reviews*, 115, 4035-4062, 10.1021/cr5006638, 2015.
- Sipilä, M., Sarnela, N., Jokinen, T., Henschel, H., Junninen, H., Kontkanen, J., Richters, S., Kangasluoma, J., Franchin, A., Peräkylä, O., Rissanen, M., Ehn, M., Vehkamäki, H., Kurten, T., Berndt, T., Petäjä, T., Worsnop, D., Ceburnis, D., Kerminen, V., ..., and O'Dowd, C.: Molecular-scale evidence of aerosol particle formation via sequential addition of HIO₃, *NATURE*, 537, 532-534, 10.1038/nature19314, 2016.
- Sjostedt, S. and Abbatt, J.: Release of gas-phase halogens from sodium halide substrates: heterogeneous oxidation of frozen solutions and desiccated salts by hydroxyl radicals, *ENVIRONMENTAL RESEARCH LETTERS*, 3, 10.1088/1748-9326/3/4/045007, 2008.
- SOLOMON, S., GARCIA, R., and RAVISHANKARA, A.: ON THE ROLE OF IODINE IN OZONE DEPLETION, *JOURNAL OF GEOPHYSICAL RESEARCH-ATMOSPHERES*, 99, 20491-20499, 1994.
- Stark, H., Yatayelli, R., Thompson, S., Kimmel, J., Cubison, M., Chhabra, P., Canagaratna, M., Jayne, J., Worsnop, D., and Jimenez, J.: Methods to extract molecular and bulk chemical information from series of complex mass spectra with limited mass resolution, *INTERNATIONAL JOURNAL OF MASS SPECTROMETRY*, 389, 26-38, 10.1016/j.ijms.2015.08.011, 2015.
- Tham, Y. J., He, X. C., Li, Q. Y., Cuevas, C. A., Shen, J. L., Kalliokoski, J., Yan, C., Iyer, S., Lehmusjarvi, T., Jang, S. H., Thakur, R. C., Beck, L., Kempainen, D., Olin, M., Sarnela, N., Mikkilä, J., Hakala, J., Marbouti, M., Yao, L., ..., and Sipilä,



M.: Direct field evidence of autocatalytic iodine release from atmospheric aerosol, *Proceedings of the National Academy of Sciences of the United States of America*, 118, 8, 10.1073/pnas.2009951118, 2021.

Wang, M., Kong, W., Marten, R., He, X., Chen, D., Pfeifer, J., Heitto, A., Kontkanen, J., Dada, L., Kurten, A., Yli-Juuti, T., Manninen, H., Amanatidis, S., Amorim, A., Baalbaki, R., Baccarini, A., Bell, D., Bertozzi, B., Bräkling, S., ..., and Donahue, N.: Rapid growth of new atmospheric particles by nitric acid and ammonia condensation, *NATURE*, 581, 184-+, 10.1038/s41586-020-2270-4, 2020.

Wang, M. Y., He, X. C., Finkenzeller, H., Iyer, S., Chen, D. X., Shen, J. L., Simon, M., Hofbauer, V., Kirkby, J., Curtius, J., Maier, N., Kurtén, T., Worsnop, D. R., Kulmala, M., Rissanen, M., Volkamer, R., Tham, Y. J., Donahue, N. M., and Sipilä, M.: Measurement of iodine species and sulfuric acid using bromide chemical ionization mass spectrometers, *Atmospheric Measurement Techniques*, 14, 4187-4202, 10.5194/amt-14-4187-2021, 2021a.

Wang, X., Jacob, D., Downs, W., Zhai, S., Zhu, L., Shah, V., Holmes, C., Sherwen, T., Alexander, B., Evans, M., Eastham, S., Neuman, J., Veres, P., Koenig, T., Volkamer, R., Huey, L., Bannan, T., Percival, C., Lee, B., and Thornton, J.: Global tropospheric halogen (Cl, Br, I) chemistry and its impact on oxidants, *ATMOSPHERIC CHEMISTRY AND PHYSICS*, 21, 13973-13996, 10.5194/acp-21-13973-2021, 2021b.

Yeoman, A., Heeley-Hill, A., Shaw, M., Andrews, S., and Lewis, A.: Inhalation of VOCs from facial moisturizers and the influence of dose proximity, *INDOOR AIR*, 32, 10.1111/ina.12948, 2022.

Zhang, Y., Liu, R., Yang, D., Guo, Y., Li, M., and Hou, K.: Chemical ionization mass spectrometry: Developments and applications for on-line characterization of atmospheric aerosols and trace gases, *TRAC-TRENDS IN ANALYTICAL CHEMISTRY*, 168, 10.1016/j.trac.2023.117353, 2023.